

MOFs for Sensing

How to cite:

International Edition: doi.org/10.1002/anie.202302645

German Edition: doi.org/10.1002/ange.202302645

Facile Synthesis of Metallosalphen-Based 2D Conductive Metal-Organic Frameworks for NO₂ Sensing: Metal Coordination Induced Planarization

Xi Su, Zhiye Zhong, Xiaoli Yan, Ting Zhang, Chuanzhe Wang, Yi-Xuan Wang,* Gang Xu,* and Long Chen*

Abstract: As an emerging class of promising porous materials, the development of two-dimensional conductive metal organic frameworks (2D *c*-MOFs) is hampered by the few categories and tedious synthesis of the specific ligands. Herein, we developed a nonplanar hexahydroxyl-functionalized Salphen ligand (6OH-Salphen) through a facile two-step synthesis, which was further applied to construct layered 2D *c*-MOFs through *in situ* one pot synthesis based on the synergistic metal binding effect of the N₂O₂ pocket of Salphen. Interestingly, the C_{2v}-symmetry of ligand endows Cu-Salphen-MOF with periodically heterogeneous pore structures. Benefitting from the higher metal density and shorter in-plane metal-metal distance, Cu-Salphen-MOF showcased excellent NO₂ sensing performance with good sensitivity, selectivity and reversibility. The current work opens up a new avenue to construct 2D *c*-MOF directly from nonplanar ligands, which greatly simplifies the synthesis and provides new possibilities for preparing different topological 2D *c*-MOF based functional materials.

Introduction

Two-dimensional conductive metal–organic frameworks (2D *c*-MOFs) are layer-stacked MOFs composed of *ortho*-substituted (–NH₂, –OH, –SH, or –SeH) conjugated building blocks (e.g., benzene, triphenylene) and square-planar coordination linkages with metal ions, which feature a graphene-like structure.^[1,2] Thanks to the strong orbital hybridization between the metal ions and ligands, as well as the open one-dimensional channel, 2D *c*-MOFs not only inherit the characteristics of traditional 3D MOFs, but also

afford specific photoelectric activity and superior conductivity, etc.^[3–7] Therefore, 2D *c*-MOFs have shown great potential applications in sensing,^[8,9] spintronics,^[7,10,11] and electrochemistry,^[12,13] among others.^[14,15] However, most reported 2D *c*-MOFs are limited to certain ligands bearing conjugated aromatic cores with high symmetries (C₃, D₂ and C₆, Figure 1), which results in 2D *c*-MOFs with few available topologies such as triangular, tetragonal and hexagonal lattices.^[16–18] Enlarging the conjugated aromatic cores could enrich the ligand family and enhance the degree of π -electron delocalization of the final 2D *c*-MOFs, but the tedious synthesis and poor solubility of the enlarged ligand in common organic solvents make the synthesis of corresponding 2D *c*-MOF great challenging. Moreover, it may reduce the density of metal sites, and thereby increase the in-plane distance between metal ions, leading to a weak communication (e.g. magnetic coupling) among neighboring metal sites. Considering the above factors, we assume that 2D *c*-MOFs might be *in situ* synthesized from nonplanar

[*] X. Su, Dr. X. Yan, Dr. T. Zhang, Dr. Y.-X. Wang, Prof. L. Chen
 Tianjin Key Laboratory of Molecular Optoelectronic Sciences,
 Department of Chemistry, School of Science, Tianjin University
 Tianjin 300072 (China)
 E-mail: yx_wang@tju.edu.cn
 long.chen@tju.edu.cn

Prof. L. Chen
 State Key Laboratory of Supramolecular Structure and Materials,
 College of Chemistry, Jilin University
 Changchun 130012 (China)
 E-mail: longchen@jlu.edu.cn

Z. Zhong
 Shanghai Key Laboratory of High-resolution Electron Microscopy &
 School of Physical Science and Technology, ShanghaiTech University
 Shanghai 201210 (China)

C. Wang, Prof. G. Xu
 State Key Laboratory of Structural Chemistry, Fujian Provincial Key
 Laboratory of Materials and Techniques toward Hydrogen Energy,
 Fujian Institute of Research on the Structure of Matter, Chinese
 Academy of Sciences
 Fuzhou, Fujian, 350002 (China)
 E-mail: gxu@fjirsm.ac.cn

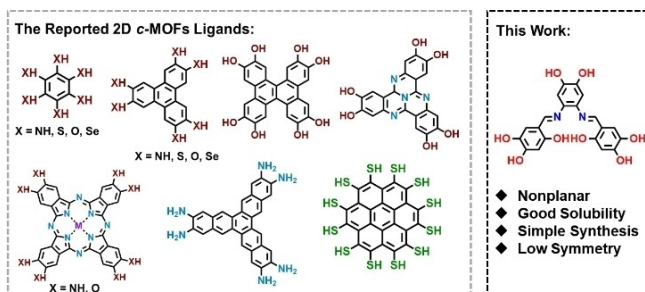


Figure 1. Representative ligands reported for 2D *c*-MOFs and the ligand studied in this work.

ligands via one-pot synthesis, where the nonplanar ligand could transform to a planar counterpart during the coordination process. In our previous work, we have proved that 2D *c*-MOF could be constructed by *in situ* oxidative cyclodehydrogenation during coordination polymerization of hydroxyl ligands.^[19] Actually, based on the preparation conditions of MOFs, metal coordination induced planarization might be an alternate to access 2D *c*-MOFs, not only simplifying the MOF synthesis, but also increasing the metal density, which is however not yet explored.

Salphen is a well-known tetradentate Schiff base ligand with C_{2v} -symmetry.^[20,21] Due to the low symmetric and nonplanar structure, Salphen and its derivatives usually possess good solubility. Notably, the N_2O_2 pocket of Salphen endows it with strong metal coordination ability with most transition metal ions under relative mild conditions.^[22,23] Upon metal coordination, the two flexible arms of Salphen are fixed to form a nearly planar structure. Therefore, to verify our hypothesis, a C_{2v} -symmetric Salphen ligand (6OH-Salphen) was newly designed and synthesized through a facile two-step synthetic route, which was further used to prepare MOF (Cu-Salphen-MOF) under solvothermal conditions. Systematical structural analysis indicated that both the N_2O_2 pocket and multitopic *ortho*-substituted functional groups of 6OH-Salphen ligand could be fully coordinated with copper ions, realizing the facile construction of layered 2D Cu-Salphen-MOF directly from nonplanar ligands. In addition, benefiting from the low symmetry of the ligand, Cu-Salphen-MOF displayed a periodically heterogeneous dual pore structures. Moreover, Cu-Salphen-MOF possessed high metal density and short in-plane metal-metal distance, thus making it display a high response toward NO_2 (100 ppm, 766 %) sensing. The current work not only broadens the categories and pore structures of 2D *c*-MOF using C_{2v} -symmetric ligands, but also opens up a new avenue to construct 2D *c*-MOF directly from nonplanar ligands, which greatly simplifies the synthesis and provides a new idea for the design 2D *c*-MOF based functional materials.

Results and Discussion

The nonplanar 6OH-Salphen was synthesized by simple condensation and further demethylation reactions (Scheme S1), which was clearly characterized by solution nuclear magnetic resonance (NMR) spectroscopy and high resolution mass spectrometry (HR-MS, Figures S5, S6, and S7). Cu-Salphen-MOF-1 was *in situ* synthesized via the coordination polymerization between copper acetate monohydrate and 6OH-Salphen ligand in a mixture of *N,N*-dimethylformamide (DMF)/deionized water (H_2O) (2/3, v/v) at 85 °C for 3 days (Scheme S2). On the other hand, the Cu-coordinated ligand (i.e. 6OH-Cu-Salphen) and the corresponding 2D *c*-MOF (Cu-Salphen-MOF-2) were synthesized for comparison (Schemes S1, S2). Notably, 6OH-Cu-Salphen exhibited much lower solubility compared to the uncoordinated 6OH-Salphen (Table S1).

Fortunately, we have obtained the single crystals of two ligand precursors (6OMe-Salphen and 6OMe-Cu-Salphen),

which could help us to better understand the structural changes before and after coordination (Figures S14, S15).^[24] As displayed in Figure 2a, 6OMe-Salphen exhibited a twisted structure whereas 6OMe-Cu-Salphen possessed a near-planar structure (Figure 2d) due to the coordination between the inner N_2O_2 pocket and copper ion. In addition, the frontier molecular orbitals further indicate that Cu-Salphen features better electron delocalization compared to the Salphen counterpart upon coordination in the inner N_2O_2 pocket (Figures 2b–f). Since the peripheral methyl-substituents have little influence on the central structures, it is inferred that the metal coordination should cause resembling structural changes of the ligand from non-planar to planar (Figure 3a).

The as-synthesized Cu-Salphen-MOF-1 and Cu-Salphen-MOF-2 were systematically characterized by various techniques. As shown in Figure S10, the Fourier transform infrared (FT-IR) spectra of the two MOFs were nearly identical, in which the stretching band of O–H ($\approx 3300\text{ cm}^{-1}$) belonging to the corresponding ligands almost disappeared and a new Cu–O ($\approx 490\text{ cm}^{-1}$) stretching vibration band appeared,

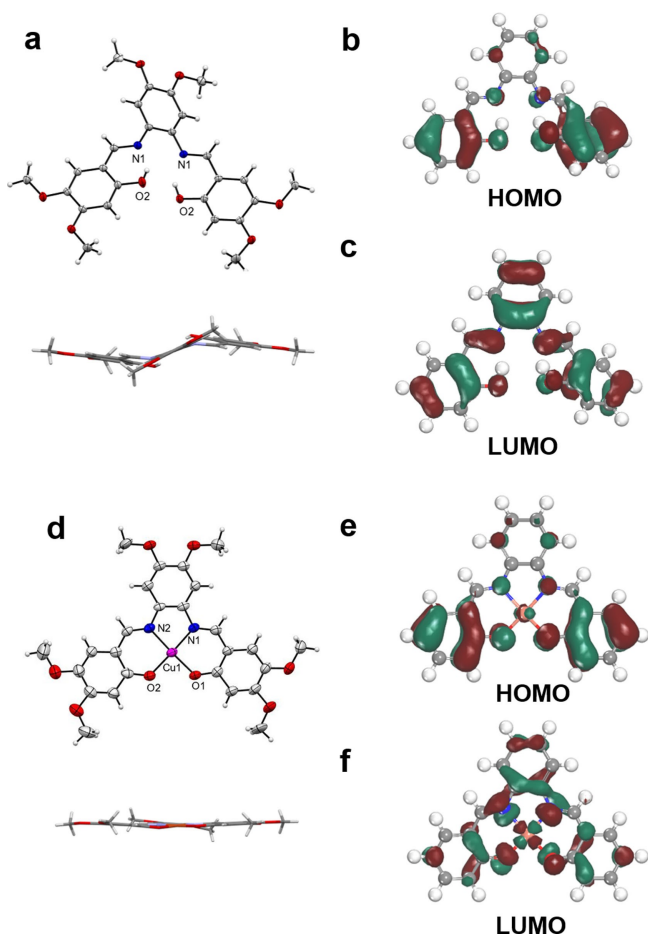


Figure 2. a) Top and side view of the single-crystal structures of non-planar 6OMe-Salphen; b) and c) HOMO and LUMO of non-planar Salphen; d) Top and side view of the single-crystal structures of near-planar Cu-Salphen; e) and f) HOMO and LUMO of near-planar Cu-Salphen (gray, carbon; blue, nitrogen; white, hydrogen; pink, copper).

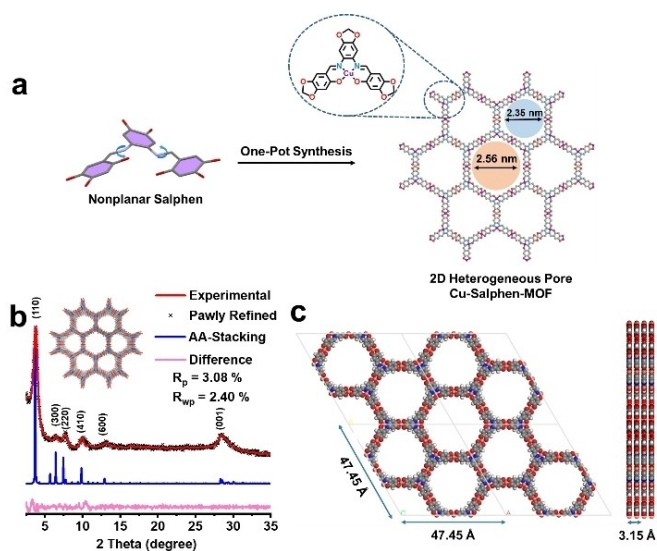


Figure 3. a) Schematic illustration of the synthesis of Cu-Salphen-MOF. b) Experimental (red), refined PXR D patterns (black dotted line) of Cu-Salphen-MOF, difference plot (pink) of experimental, AA stacking simulation and refined PXR D pattern. c) Top-view and side-view for AA stacking model of Cu-Salphen-MOF.

confirming the occurrence of metal coordination. Notably, the new characteristic Cu–O and Cu–N ($\approx 560\text{ cm}^{-1}$) stretching band appearing in 6OH-Cu-Salphen complex and Cu-Salphen-MOF-2, were also observed in Cu-Salphen-MOF-1, indicating that the inner N_2O_2 pocket of the nonplanar 6OH-Salphen also coordinated with copper ions during the solvothermal synthesis. As the elemental analysis results of the two MOFs are almost identical, nearly all of inner N_2O_2 pockets in the Salphen were coordinated with Cu^{2+} , leading to a planar structure. In addition, the powder X-ray diffraction (PXR D) patterns of the both MOFs were nearly identical, which further confirmed the above conclusion (Figure S16). As both 2D *c*-MOFs possessed the same structure, whereas Cu-Salphen-MOF-1 can be more facile obtained in terms of synthesis, therefore Cu-Salphen-MOF-1 was selected as representative for further analysis, which termed as Cu-Salphen-MOF in the following discussion for convenience. The successful coordination of metal into the inner N_2O_2 pocket lead to a higher metal density and a short metal-metal distance. As revealed by inductively coupled plasma emission spectroscopy (ICP), the metal (Cu) content of the as-prepared MOF was 28.37%, which is close to the theoretical value of Cu-Salphen-MOF (27.53%), further demonstrating the successful and complete coordination in the N_2O_2 pocket. The in-plane distance between the N_2O_2 pocket coordinated Cu and the outside catecolate coordinated Cu was only 7.7 Å.

The crystalline structure of Cu-Salphen-MOF was characterized by PXR D and high-resolution transmission electron microscopy (HRTEM). In the PXR D pattern of Cu-Salphen-MOF (Figure 3b), an intense diffraction peak was observed at 3.80° corresponding to (110) lattice plane, together with some minor peaks at 6.45° , 7.75° , 10.10° , 13.20° and 28.40° , which could be indexed to 300, 220, 410, 600 and

001, respectively. The simulated PXR D pattern of Cu-Salphen-MOF with AA stacking and periodically heterogeneous pore structures using Materials Studio software showed a good agreement with the experimental one compared to that with AB stacking or ABC stacking manner (Figure S17).^[25] Pawley refinement afforded the P_6 space group with the cell parameters of $a = 47.45\text{ \AA}$ and $c = 3.15\text{ \AA}$ ($R_{\text{wp}} = 2.40\%$, $R_p = 3.08\%$). HRTEM images displayed clear lattice fringes of (110) and (001) planes throughout the whole crystallites with $d_{110} = 23.2\text{ \AA}$ and $d_{001} = 3.15\text{ \AA}$, which were roughly consistent with the structure with the AA stacking (Figures 4c, d and S22). Notably, due to the low symmetry of the ligand, the as-prepared MOF displayed periodically heterogeneous dual pore structures. Scanning electron microscope (SEM) images of Cu-Salphen-MOF revealed a spherical morphology (Figures 4a and S21).

The permanent porosity of Cu-Salphen-MOF was assessed through nitrogen sorption measurements at 77 K. As shown in Figure 4b, a Brunauer–Emmett–Teller (BET) surface area of $450\text{ m}^2\text{ g}^{-1}$ was calculated from the N_2 adsorption branch ($P/P_0 < 0.15$). Based on the nonlocal density functional theory (NLDFT) method, the pore size distribution of Cu-Salphen-MOF was estimated to be 2.50 nm. The calculated value was consistent with the theoretical diameter of the simulated periodically heterogeneous pore structures (2.35 and 2.56 nm). The ultraviolet-visible (UV/Vis) spectra and ultraviolet photoelectron spectroscopy (UPS) of Cu-Salphen-MOF showed a broad absorption band, demonstrating its large extended π -conjugation (Figures S11b and S13). Accordingly, the optical band gap was calculated to be 1.26 eV, indicating a semiconductor character. To further verify the effect of planarization on the electronic structure of Cu-Salphen-MOF, DFT calculations were conducted to compare the energy band structures of the planar Cu-Salphen-MOF and its counterpart (twisted Cu-Salphen-MOF without metal in the N_2O_2 pockets of Salphen, Figure S25). The results indicated that

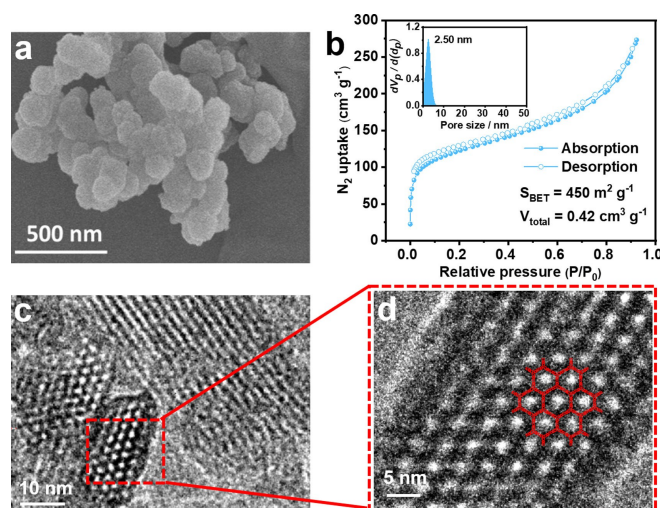


Figure 4. a) SEM image of Cu-Salphen-MOF. b) N_2 adsorption-desorption isotherms (77 K) and pore-size distribution of Cu-Salphen-MOF. c), d) TEM images of Cu-Salphen-MOF.

the band gap of the planarized Cu-Salphen-MOF was only 1.02 eV, which was similar to the experimental value, while the twisted one displayed a larger band gap (1.49 eV, Figures S5d and S26). In addition, the electrical conductivities at different temperatures were measured by two-probe method, and the results showed that the conductivity increased nonlinearly with the increase of temperature, which was a typical semiconductor character (Figures 5a and b). The above results further demonstrated that the occurrence of metal induced planarization was beneficial to reduce the band gap and promote the carrier transport (Figures S27 and S28).

Nitrogen dioxide (NO_2) is one of the typical global pollutants and very toxic even at low concentrations. 2D *c*-MOFs with good conductivity is emerging as promising sensor for NO_2 , however it is still in its infancy.^[26–29] On the other hand, metal ions have been reported to be very effective active sites for NO_2 sensing.^[30] As a result, inspired by the high metal density and short metal spacing of Cu-Salphen-MOF, we speculated that both the responsivity and sensitivity would be improved if Cu-Salphen-MOF was applied for NO_2 sensing. To verify our hypothesis, Cu-Salphen-MOF was deposited on the interdigitated electrodes by drop casting, and the current signals of the device were recorded under NO_2 atmosphere. The accuracy of the test results was ensured by preparing two devices for the same sample in parallel. All tests were conducted under dark at room temperature, and the relative current variation before and after exposure to NO_2 gas was defined as device

responsivity. As shown in Figures 5e and S29a, Cu-Salphen-MOF displayed good response-recovery ability in a broad concentration range of NO_2 (1–100 ppm), and the response coefficient of variation (CV) was only 3.4% over five continuous cycles (10 ppm), indicating its excellent repeatability and reliability. In addition, the PXRD pattern and N_2 adsorption-desorption isotherm of Cu-Salphen-MOF maintained after NO_2 sensing tests (Figure S31), demonstrating its excellent stability under the NO_2 atmosphere. In Figure S29b, the log-log plot of response concentration of Cu-Salphen-MOF revealed an excellent linear relationship in the range of 1–100 ppm. The theoretical limit of detection (LOD) fitted linear equation was calculated to be 0.28 ppm by setting the response value to 10%. Besides, the response time (t_{res} : defined as the time achieved for increasing the current to 90% of the maximum signal) of Cu-Salphen-MOF upon exposure to 10 ppm NO_2 was evaluated (Figure S29c). The t_{res} of Cu-Salphen-MOF (2.25 min) was relatively short, which could be attributed to the rapid adsorption of NO_2 by densely arranged copper active sites distributed in the 1D channels. Compared with other representative MOF based sensors (Table S4), Cu-Salphen-MOF featured a high NO_2 response and a low detection limit.

Selectivity is another essential parameter to evaluate sensing performance. Therefore, Cu-Salphen-MOF was exposed to twelve different kinds of interfering gases at the concentration of 100 ppm for 3 min as comparison (Figure 5f). Notably, it showed very weak responses (< 25%)

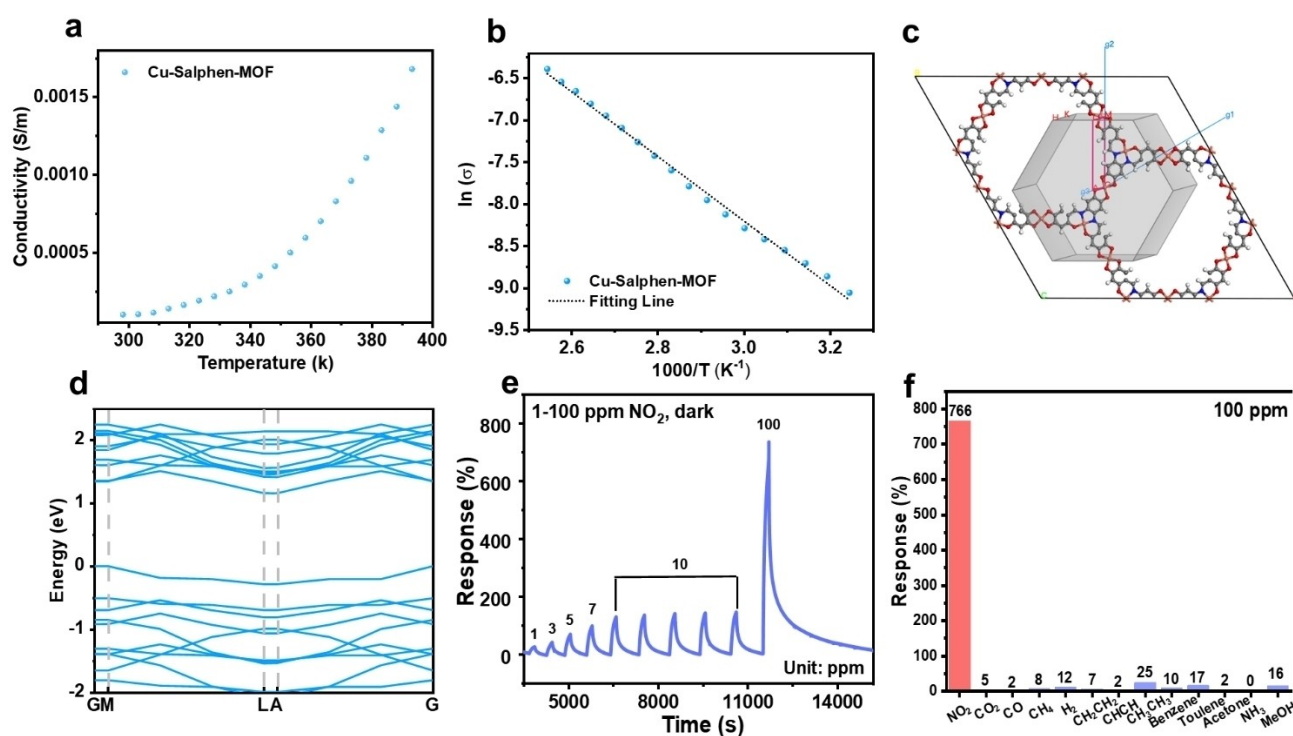


Figure 5. a) Variable-temperature conductivity for Cu-Salphen-MOF. b) Arrhenius fitting of temperature-dependent conductivity data for Cu-Salphen-MOF. c) Unit cell of Cu-Salphen-MOF and its first Brillouin zone. d) Calculated electronic band structure of the planarized Cu-Salphen-MOF. e) Dynamic response curves toward 1–100 ppm NO_2 . f) Response value to 12 types of gases (100 ppm).

toward these interference gases, indicating that Cu-Salphen-MOF could well distinguish NO₂ from common interference gases. To evaluate the interference of water vapor in the environment, the response of Cu-Salphen-MOF to NO₂ under different humidity levels was tested. As displayed in Figure S34, compared with that in dry air, Cu-Salphen-MOF shows higher sensing response towards NO₂ in the presence of water vapor, suggesting the selectivity of the MOF towards NO₂ is affected by water. Moreover, Cu-Salphen-MOF displayed a long-term stability in response to NO₂ as no obvious changes in current value were observed after 10 days (Figure S29d). To explore the mechanism, the XPS and adsorption energy measurements were conducted. These results revealed that the NO₂ response could be attributed to the redox effect of abundant copper ions. Among them, the copper ions on the N₂O₂ pocket exhibited a greater adsorption energy and activity (Details see the Section 13 in the Supporting Information).

Conclusion

In summary, a new nonplanar Salphen ligand (6OH-Salphen) with C_{2v}-symmetry was developed to construct 2D MOF (Cu-Salphen-MOF) via *in situ* one pot synthesis, featuring a metal coordination induced planarization of the Salphen cores. Benefiting from the low symmetry of the ligand, the as-prepared 2D *c*-MOF adopted periodically heterogeneous dual pore structures. Moreover, the existence of N₂O₂ pocket of 6OH-Salphen endows the Cu-Salphen-MOF with higher metal density, shorter metal-metal distance and a narrower band gap, thus making it display a high response toward NO₂. Our current work not only enrich the topological structures, but also opens up a new avenue to construct 2D *c*-MOF directly from nonplanar ligands, which could greatly simplify the synthesis and provides a new idea for the design of 2D *c*-MOFs. Further functionalization of other coordination groups (e.g. -SH, -NH₂) on the Salphen motif and variation of the metal centers are currently in progress in our laboratory, which could expect interesting properties in catalysis, energy storage/conversion, among others.

Acknowledgements

This work was financially supported by National Natural Science Foundation of China (51973153) and the National Key Research and Development Program of China (2017YFA0207500). G.X. is grateful for the financial supports from National Natural Science Foundation of China (22171263), Scientific Research and Equipment Development Project of CAS (YJKYQ20210024). The authors thank Prof. Yanhang Ma at ShanghaiTech University for his scientific discussions.

Conflict of Interest

The authors declare no conflict of interest.

Data Availability Statement

The data that support the findings of this study are available in the Supporting Information of this article.

Keywords: Conjugated Metal–Organic Framework · Heterogeneous Pore · Higher Metal Density · NO₂ Sensing

- [1] M. Wang, R. Dong, X. Feng, *Chem. Soc. Rev.* **2021**, *50*, 2764–2793.
- [2] J. Liu, X. Song, T. Zhang, S. Liu, H. Wen, L. Chen, *Angew. Chem. Int. Ed.* **2021**, *60*, 5612–5624.
- [3] M. Ko, L. Mendecki, K. A. Mirica, *Chem. Commun.* **2018**, *54*, 7873–7891.
- [4] Z. Meng, R. M. Stolz, L. Mendecki, K. A. Mirica, *Chem. Rev.* **2019**, *119*, 478–598.
- [5] L. S. Xie, G. Skorupskii, M. Dincă, *Chem. Rev.* **2020**, *120*, 8536–8580.
- [6] W.-T. Koo, J.-S. Jang, I.-D. Kim, *Chem* **2019**, *5*, 1938–1963.
- [7] C. Yang, R. Dong, M. Wang, P. S. Petkov, Z. Zhang, M. Wang, P. Han, M. Ballabio, S. A. Bräuninger, Z. Liao, J. Zhang, F. Schwotzer, E. Zschech, H.-H. Klaus, E. Cánovas, S. Kaskel, M. Bonn, S. Zhou, T. Heine, X. Feng, *Nat. Commun.* **2019**, *10*, 3260.
- [8] M. G. Campbell, D. Sheberla, S. F. Liu, T. M. Swager, M. Dincă, *Angew. Chem. Int. Ed.* **2015**, *54*, 4349–4352.
- [9] M.-S. Yao, X.-J. Lv, Z.-H. Fu, W.-H. Li, W.-H. Deng, G.-D. Wu, G. Xu, *Angew. Chem. Int. Ed.* **2017**, *56*, 16510–16514.
- [10] R. Dong, Z. Zhang, D. C. Tranca, S. Zhou, M. Wang, P. Adler, Z. Liao, F. Liu, Y. Sun, W. Shi, Z. Zhang, E. Zschech, S. C. B. Mannsfeld, C. Felser, X. Feng, *Nat. Commun.* **2018**, *9*, 2637.
- [11] X. Song, X. Wang, Y. Li, C. Zheng, B. Zhang, C.-a. Di, F. Li, C. Jin, W. Mi, L. Chen, W. Hu, *Angew. Chem. Int. Ed.* **2020**, *59*, 1118–1123.
- [12] E. M. Miner, T. Fukushima, D. Sheberla, L. Sun, Y. Surendranath, M. Dincă, *Nat. Commun.* **2016**, *7*, 10942.
- [13] D. Sheberla, J. C. Bachman, J. S. Elias, C.-J. Sun, Y. Shao-Horn, M. Dincă, *Nat. Mater.* **2017**, *16*, 220–224.
- [14] H. Arora, R. Dong, T. Venanzi, J. Zscharschuch, H. Schneider, M. Helm, X. Feng, E. Cánovas, A. Erbe, *Adv. Mater.* **2020**, *32*, 1907063.
- [15] X. Huang, P. Sheng, Z. Tu, F. Zhang, J. Wang, H. Geng, Y. Zou, C.-a. Di, Y. Yi, Y. Sun, W. Xu, D. Zhu, *Nat. Commun.* **2015**, *6*, 7408.
- [16] B. Wang, J. Li, M. Ye, Y. Zhang, Y. Tang, X. Hu, J. He, C. C. Li, *Adv. Funct. Mater.* **2022**, *32*, 2112072.
- [17] Z. Meng, A. Aykanat, K. A. Mirica, *J. Am. Chem. Soc.* **2019**, *141*, 2046–2053.
- [18] X. Huang, S. Zhang, L. Liu, L. Yu, G. Chen, W. Xu, D. Zhu, *Angew. Chem. Int. Ed.* **2018**, *57*, 146–150.
- [19] M. Qi, Y. Zhou, Y. Lv, W. Chen, X. Su, T. Zhang, G. Xing, G. Xu, O. Terasaki, L. Chen, *J. Am. Chem. Soc.* **2023**, *145*, 2739–2744.
- [20] E. N. Jacobsen, *Acc. Chem. Res.* **2000**, *33*, 421–431.
- [21] P. Pfeiffer, E. Breith, E. Lübbe, T. Tsumaki, *Justus Liebigs Ann. Chem.* **1933**, *503*, 84–130.
- [22] C. J. Whiteoak, G. Salassa, A. W. Kleij, *Chem. Soc. Rev.* **2012**, *41*, 622–631.

- [23] C. Freire, M. Nunes, C. Pereira, D. M. Fernandes, A. F. Peixoto, M. Rocha, *Coord. Chem. Rev.* **2019**, *394*, 104–134.
- [24] Deposition Numbers 2215370 and 2119809 contain the supplementary crystallographic data for this paper. These data are provided free of charge by the joint Cambridge Crystallographic Data Centre and Fachinformationszentrum Karlsruhe Access Structures service.
- [25] Z. Yang, J. Liu, Y. Li, G. Zhang, G. Xing, L. Chen, *Angew. Chem. Int. Ed.* **2021**, *60*, 20754–20759.
- [26] Y. Lin, W.-H. Li, Y. Wen, G.-E. Wang, X.-L. Ye, G. Xu, *Angew. Chem. Int. Ed.* **2021**, *60*, 25758–25761.
- [27] A. Aykanat, Z. Meng, R. M. Stolz, C. T. Morrell, K. A. Mirica, *Angew. Chem. Int. Ed.* **2022**, *61*, e202113665.
- [28] Y. Yue, P. Cai, X. Xu, H. Li, H. Chen, H.-C. Zhou, N. Huang, *Angew. Chem. Int. Ed.* **2021**, *60*, 10806–10813.
- [29] A.-Q. Wu, W.-Q. Wang, H.-B. Zhan, L.-A. Cao, X.-L. Ye, J.-J. Zheng, P. N. Kumar, K. Chiranjeevulu, W.-H. Deng, G.-E. Wang, M.-S. Yao, G. Xu, *Nano Res.* **2021**, *14*, 438–443.
- [30] M. Liu, Y.-J. Chen, X. Huang, L.-Z. Dong, M. Lu, C. Guo, D. Yuan, Y. Chen, G. Xu, S.-L. Li, Y.-Q. Lan, *Angew. Chem. Int. Ed.* **2022**, *61*, e202115308.

Manuscript received: February 21, 2023

Accepted manuscript online: March 23, 2023

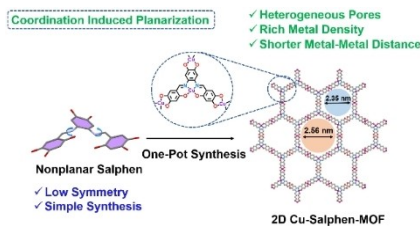
Version of record online: ■■■, ■■■

Research Articles

MOFs for Sensing

X. Su, Z. Zhong, X. Yan, T. Zhang, C. Wang,
Y.-X. Wang,* G. Xu,*
L. Chen* **e202302645**

Facile Synthesis of Metallosalphen-Based
2D Conductive Metal-Organic Frameworks
for NO₂ Sensing: Metal Coordination In-
duced Planarization



A new nonplanar Salphen ligand (6OH-Salphen) with C_{2v}-symmetry was developed to construct 2D Cu-Salphen-MOF via *in situ* one pot synthesis, featuring metal coordination induced planarization of the Salphen cores. The existence of N₂O₂ pocket of 6OH-Salphen endows 2D Cu-Salphen-MOF with higher metal density, shorter metal-metal distance and a narrower band gap, thus making it display a high response toward NO₂ (766% at 100 ppm).